biology and life sciences forum

MDPI

Proceeding Paper

Bioactive Profiling of *Citrus aurantium* Peel Ethanol Extract and Effects on *Escherichia coli* and *Staphylococcus aureus* Drug Target Proteins †

Kehinde Oluyemi Ajayi [1,2,*], Bisola Kemi Olaoye [1], Blessing Tolulope Owolabi [3,4] and Timothy O. Adejumo [1]

[1] Microbiology Unit, Department of Natural Science, Precious Cornerstone University, Ibadan 6576, Nigeria; olaoyebisolak@yahoo.com (B.K.O.); timothy.adejumo@pcu.edu.ng (T.O.A.)
[2] Center for Research Innovations and Discoveries, Precious Cornerstone University, Ibadan 6576, Nigeria
[3] Department of Physiology, Faculty of Basic Medical Sciences, College of Medicine, Ekiti State University, Ado Ekiti 5363, Nigeria; owolabi.b.1903003112@eksu.edu.ng
[4] Department of Pharmacology and Therapeutics, University of Ibadan, Ibadan 22133, Nigeria
* Correspondence: ajayikehinde@pcu.edu.ng; Tel.: +234-703-899-0588
† Presented at the 1st International Online Conference on Biology (IOCBI 2026), 10–12 February 2026; Available online: https://sciforum.net/event/IOCBI2026.

Abstract

The rising threat of antimicrobial resistance necessitates the search for novel bioactive molecules from natural sources. This study investigated the phytochemical composition, antibacterial potency, and molecular docking interactions of *Citrus aurantium* peel ethanol extract against *Escherichia coli* outer-membrane and topoisomerase proteins and *Staphylococcus aureus* toxins as drug target proteins. Qualitative and quantitative phytochemical compositions were examined using standard analytical methods, chemical compounds were evaluated and qualified using Gas Chromatography–Mass Spectrometry (GC-MS), and antibacterial effects were investigated in silico and validated in vitro. Qualitative and quantitative analyses revealed high concentrations of flavonoids (4.54 ± 0.11%), alkaloids (1.6 ± 0.03%), terpenoids (1.35 ± 0.01%), tannins (1.02 ± 0.05%), phenols (0.97 ± 0.07%), and saponins (0.80 ± 0.01%). GC–MS profiling identified several dominant compounds, including β-D-glucopyranose, neo-inositol, 8-(2,3-dihydroxy-3-methylbutyl)-7-methoxy-2H-chromen-2-one, and D-allose. In silico docking studies against bacterial druggable proteins (PDB IDs: 4C56 and 3MFG, which are *S. aureus* toxins; 1BXW and 3FV5, which are *E. coli* outer-membrane and topoisomerase proteins) revealed strong binding affinities (−6.477 to −8.774 kcal/mol), comparable to standard antibiotics. ADMET predictions confirmed favorable pharmacokinetic and safety profiles, with most lead compounds displaying high intestinal absorption, low hepatotoxicity, and compliance with Lipinski's rule of five. The extract exhibited stronger antibacterial activity, producing inhibition zones of 25.11 ± 0.017 and 23.04 ± 0.25 mm against clinical isolates of *S. aureus* and *E. coli*, respectively, at a concentration of 10 mg/mL, comparable to ciprofloxacin (30.35 ± 0.26 mm). These findings highlight *C. aurantium* peel phytoconstituents as promising scaffolds for antibacterial drug development and justify further in vivo validation for combating multidrug-resistant pathogens.

Keywords: GC-MS; phytochemicals; antibacterial; extract; toxins; outer membrane; topoisomerase

Check for updates

Academic Editor: Andrés Moya

Published: 25 May 2026

Copyright: © 2026 by the authors. Licensee MDPI, Basel, Switzerland. This article is an open access article distributed under the terms and conditions of the Creative Commons Attribution (CC BY) license.

1. Introduction

Antimicrobial resistance (AMR) ranks among the most pressing threats to global public health and development. In 2019, bacterial AMR was estimated to have directly caused 1.27 million deaths worldwide, while contributing to approximately 4.95 million deaths and higher healthcare costs [1]. A major force driving the AMR crisis is the indiscriminate and excessive application of antimicrobials in human medicine, crop agriculture, and animal husbandry [2]. The increasingly globalized nature of the food trade exacerbates this problem by enabling drug-resistant strains to spread beyond national borders, escalating what may begin as contained outbreaks into public health emergencies of global concern [3,4].

Clinically important pathogens such as *Escherichia coli* and *Staphylococcus aureus* are increasingly developing resistance to commonly used drugs, thereby necessitating the exploration of alternative therapeutic agents. Bacterial proteins, such as outer-membrane proteins and DNA topoisomerases in *E. coli*, as well as virulence-associated toxins in *S. aureus*, are drug targets because of their crucial roles in bacterial survival, replication, structural integrity, and pathogenicity. Targeting these proteins offers a strategic approach to disrupting bacterial growth and virulence.

Natural product-derived antimicrobials, especially plant-derived phytochemicals, have gained considerable attention as promising sources of novel bioactive compounds with diverse pharmacological properties in the fight against AMR. *Citrus aurantium* (bitter orange) peel has a rich content of bioactive compounds, including multiple phenolic acids and flavonoids which are capable of exhibiting antimicrobial activity [5]. However, despite its established ethnomedicinal relevance, there is a paucity of comprehensive studies integrating phytochemical profiling, in silico molecular docking against defined bacterial drug targets, and in vitro validation, hence the need for this study.

2. Materials and Methods

2.1. Collection of Citrus aurantium

Mature fruits of *Citrus aurantium* L. (bitter orange) were collected from healthy trees during the peak fruiting season (November–February) from Ola-Ogun Area, Ibadan, Nigeria. The fruits were identified and authenticated by a botanist at the University of Ibadan and a voucher specimen (PLM/2025/XL/016) was deposited at the institutional herbarium for reference. The collected fruits were thoroughly washed under running tap water, followed by rinsing with distilled water to remove surface contaminants, dirt, and microbial load. The fruits were manually peeled using a sterile stainless-steel knife, and the peels (exocarp) were separated. The fresh peels were cut into small uniform pieces (approximately 1–2 cm^2) and spread in single layers on clean stainless-steel trays. Drying was carried out in a hot-air oven at 40–45 °C for 48–72 h until a constant weight was achieved. The dried peels were then ground into a fine powder using an electric grinder and sieved through a mesh (particle size $\leq$ 0.5 mm) to obtain a homogenous powder. The powdered material was stored in airtight, light-protected containers at 4 °C until further use [5].

2.2. Ethanol Extraction of Bioactive Compounds in C. aurantium Peels

The ethanolic extract was prepared using the maceration method. Approximately 50 g of the dried peel powder was soaked in 500 mL of 95% (*v*/*v*) ethanol in a conical flask (ratio 1:10, *w*/*v*). The mixture was agitated intermittently on a magnetic stirrer and allowed to macerate at room temperature (25 $\pm$ 2 °C) for 72 h. The resulting mixture was filtered through Whatman No. 1 filter paper, and the residue was re-extracted twice under the same conditions to ensure maximum recovery of bioactive compounds. The filtrates were pooled and concentrated under reduced pressure using a rotary vacuum evaporator (at

40 °C) to remove the solvent [6]. The crude extract was then transferred to pre-weighed glass vials, dried to a semi-solid consistency, and stored at 4 °C in the dark until use.

2.3. Quantitative Phytochemical Screening

The crude ethanolic extract was subjected to standard quantitative phytochemical tests to detect the presence of major classes of bioactive compounds, following standard methods described by [5], to determine various phytochemical components such as phenols, glycosides, saponins, flavonoids, alkaloids, and tannins.

2.4. Gas Chromatography–Mass Spectroscopic Analysis of Citrus aurantium Peel Extract

GC-MS analysis of Citrus aurantium peel extract was conducted using a Thermo GC-Trace Ultra equipped with a DB 35-MS capillary column (30 mm × 0.25 mm × 0.25 µm) Varian 3800/4000, San Diego, CA, USA. Helium served as the carrier gas at 1.0 mL/min. Components were identified by comparing mass spectra against NIST and Wiley library databases [7].

2.5. Bacterial Strains

The characterized multidrug-resistant *Escherichia coli* (MCB0168) and *Staphylococcus aureus* (MCB0311) maintained in the Precious Cornerstone University, Ibadan, Natural Science Departmental laboratory repository culture were re-validated using PCR assays [8], which were used to evaluate the in vitro antibacterial efficacy of the extract.

2.6. In Silico Assays

2.6.1. Selection of Protein Motifs

The chemical structures of the identified phytochemical ligands retrieved from the PubChem-NCBI database were drawn using Chem 3D v.16.0 software. The protein motifs of *S. aureus* Enterotoxin B and Toxic Shock Syndrome Toxin-1 (PDB IDs: 4C56 and 3MFG) and *E. coli* outer-membrane and topoisomerase proteins (1BXW and 3FV5) were selected from the protein data bank (PDB).

2.6.2. In Silico Absorption, Distribution, Metabolism, Excretion, and Toxicity (ADMET) Analysis and Molecular Docking Using Autodock v.4.20

The pharmacokinetic and toxicity profiles of identified phytochemicals were evaluated using in silico ADMET analysis. The SwissADME server was employed to predict physicochemical properties, lipophilicity, water solubility, pharmacokinetics, and drug-likeness. Toxicity was assessed using ProTox-II, which predicted LD_{50} values and toxicity classes, and StopTox, which evaluated cardiotoxicity through hERG liability prediction. Molecular docking was performed using AutoDock v.4.20 to determine the binding affinity of phytochemical ligands against target proteins. Low-energy 3D ligand conformations were generated using Chem3D v.16.0. Target proteins were prepared by removing water molecules, heteroatoms, and co-crystallized solvents, followed by the addition of Gasteiger charges and polar hydrogens. A grid map (60 × 60 × 60 points, 0.375 Å spacing) was generated, and the Lamarckian genetic algorithm produced the ten best-ranked poses per ligand. Docking results were visualized using PyMOL Version 3.0 [9,10].

2.7. In Vitro Antibacterial Activity of Extract Using Agar Well Diffusion Assay

The antibacterial activities of the extract were determined by agar well diffusion assay techniques [11]. In this method, 100 µL of standardized inoculum (1×10^6 cfu/mL) of each test bacterium was spread onto sterile Muller–Hinton Agar. A well of 8 mm diameter was cut from the agar using a sterile cork-borer; subsequently, each well was filled with 100 µL of different concentrations of extract, and ciprofloxacin antibiotic was used as a

positive control. The plates were kept at room temperature for 1 h to allow proper diffusion of the extract into agar and then incubated at 37 °C for 24 h. Triplicates were prepared for each sample. The extracts with antibacterial activity inhibited the microbial growth and clear zones were formed. The diameter of the zone of inhibition was measured in millimeters [12].

3. Results and Discussion

3.1. Quantitative Phytochemical Composition and GC–MS Spectral Analysis

The quantitative phytochemical analysis of the ethanolic peel extract of *Citrus aurantium* (Table 1) revealed that flavonoids were the most abundant phytochemical, with a value of 4.54 ± 0.11% (*w*/*w*), followed by alkaloids (1.60 ± 0.003%) and terpenoids (1.35 ± 0.001%). Tannins and phenolic compounds were present at 1.02 ± 0.005% and 0.97 ± 0.007%, respectively. Saponins had the lowest concentration among the quantified constituents, with a value of 0.80 ± 0.001%. The higher concentration of flavonoids corroborates [5], who identified constituents in *C. aurantium* peels via HPLC. The higher flavonoid recovery in our ethanolic extract compared to their aqueous preparation reflects ethanol's superior capacity for solubilizing both glycosylated and aglycone flavonoids [13]. Alkaloid and saponin contents align with the qualitative detection of berberine and saponins reported by [5]. The moderate alkaloid and terpenoid contents suggest potential antimicrobial and anti-inflammatory activities, while tannins, phenolics, and saponins may contribute synergistically to overall bioactivity [14].

Table 1. Quantitative phytochemical composition of ethanolic extract of *Citrus aurantium* peels.

Parameters	Ethanol Extract (%*w*/*w*)
Alkaloids	1.6 ± 0.003
Flavonoids	4.54 ± 0.11
Phenol	0.97 ± 0.007
Saponins	0.80 ± 0.001
Tannins	1.02 ± 0.005
Terpenoids	1.35 ± 0.001

GC–MS profiling (Figure 1 and Table 2) revealed 25 compounds, with hexanoic acid (19.79%), chromene derivatives (13.89%), and isoauraptene (6.32%) as notable constituents. The detection of coumarin-related compounds corroborates the qualitative identification of coumarins reported by Hadi [5]. Minor constituents including D-allose derivatives and 2-methoxy-4-vinylphenol may offer additional bioactivities, showing that the phytochemical richness of *C. aurantium* peels could be explored as antimicrobial lead compounds.

Table 2. GCMS spectra analysis of *C. aurantium* peel extract.

Peak Number	Real Time	Area (%)	Name of Compounds
1	3.431	2.81	Phenol, N-Acrylonitrylaziridine, Benzene, ethoxy-
2	3.820	2.71	4(H)-Pyridine, N-acetyl-3-Cyclohexene-1-acetaldehyde 1,3-Diazine
3	4.134	1.01	2-Propenal, 3-(dimethylamino)-3-(1-piperidinyl) Aziridine, 2,2,3,3-tetramethyl-1,2-Dimethylpyrrolidine
4	4.804	2.75	Benzoic acid, methyl ester
5	4.970	1.42	3-Tridecanol 2-Furanmethanol, 5-ethenyltetrahyd ro-.alpha.,.alpha.,5-trimethyl-, c is- 4,5-Dimethyl-3-heptanol
6	6.406	1.19	4-Methyleneisophorone 2,4-Cycloheptadien-1-one, 2,6,6-trimethyl-
7	7.442	2.12	2-Methoxy-4-vinylphenol 3-Methoxyacetophenone Ethanone, 1-(2-hydroxy-5-methylphenyl)-

Table 2. *Cont.*

Peak Number	Real Time	Area (%)	Name of Compounds
8	8.929	1.60	Tricyclo[3.1.0.0(2,4)]hexane, 3,3,6,6-tetramethyl-, (1.alpha.,2.beta.,4.beta.,5.alpha.) Thiocyanic acid, 4-oxotricyclo[3.3.1.1(3,7)]dec-2-yl ester,
9	9.462	3.46	(1.alpha.,2.alpha.,3.beta.,5.alpha.,7.beta.) 2,6-Dimethyl-3,5,7-octatriene-2-ol, ,E,E D-Allose.beta.-D-Glucopyranose, 1,6-anhydro 3,4-Altrosan
10	9.736	3.78	4-Cyclopropylmethylbenzonitrile 6-Methyl benzobicyclo[2.2.1] hepte none-5 N,N′-(1,2-Propylene)-thiourea
11	10.446	1.77	Methyl-.beta.-D-thiogalactoside.beta.-D-Glucopyranoside, methyl.alpha.-D-Glucopyranoside, methyl
12	10.823	19.79	Hexanoic acid, Pentanoic acid
13	11.029	1.10	Indole, 3-methyl- Methylcyclohexanol, (E)-, TMS derivative, Tryptamine
14	11.224	1.30	.beta.-Allyloxypropionic acid, D-Galactose, Morpholine, 4-methyl-, 4-oxide
15	12.260	1.84	D-glycero-D-gulo-Heptonic acid,.delta.-lactone Lactose.alpha.-D-Glucopyranose, 4-O-.beta.-D-galactopyranosyl
16	12.729	2.57	Scyllo-Inositol, Neo-Inositol, l-Inositol
17	13.345	1.81	Hexadecanoic acid, methyl ester Pentadecanoic acid, 14-methyl-, methyl ester
18	13.736	1.86	n-Hexadecanoic acid
19	15.063	16.57	Formamidine, N′-(m-acetylphenyl)-N,N-dimethyl Pyrimidine, 6-oxo-4-(3-fluoropheny l)-1,6-dihydro Phenol, 4-(2-thienylmethyl)-
20	15.321	1.50	acetamide, N-[4-(dimethylamino)phenyl] 2-Thiazolamine, 4,5-dihydro-N-phenyl 1-(3-Ethoxyphenyl)acetone
21	15.865	6.32	Isoauraptene [1,2,4]Triazolo[4,3-b]cinnolin-10-ol, 6,7,8,9-tetrahydro 8H-Cyclopenta[d][1,2,4]triazolo[1, 5-a]pyrimidin-8-one, 4,5,6,7-tetra hydro-2-methyl
22	16.288	2.59	Auraptenol Pyrazol-5(4H)-one, 3-(4-methoxyphenyl)-[1,2,4]Triazolo[4,3-b]cinnolin-10-ol, 6,7,8,9-tetrahydro-
23	16.660	3.20	Thiophene, 2,2′-(1,2-ethenediyl)bis-, (E)-1H-1,3-Benzimidazole-2-methanol, 5-methoxy-1-methyl Anthracene, 9-methyl-
24	17.507	1.02	Squalene, 1,5,9-Undecatriene, 2,6,10-trimethyl, (Z)-
25	17.856	13.89	8-(2,3-Dihydroxy-3-methylbutyl)-7-methoxy-2H-chromen-2-one, N-Cyclohexylidene-2-carbamylcyclohex-1-enylamine, 6-Chloro-3-methyl-1,2,3,4-tetrahydro-.gamma.-carboline

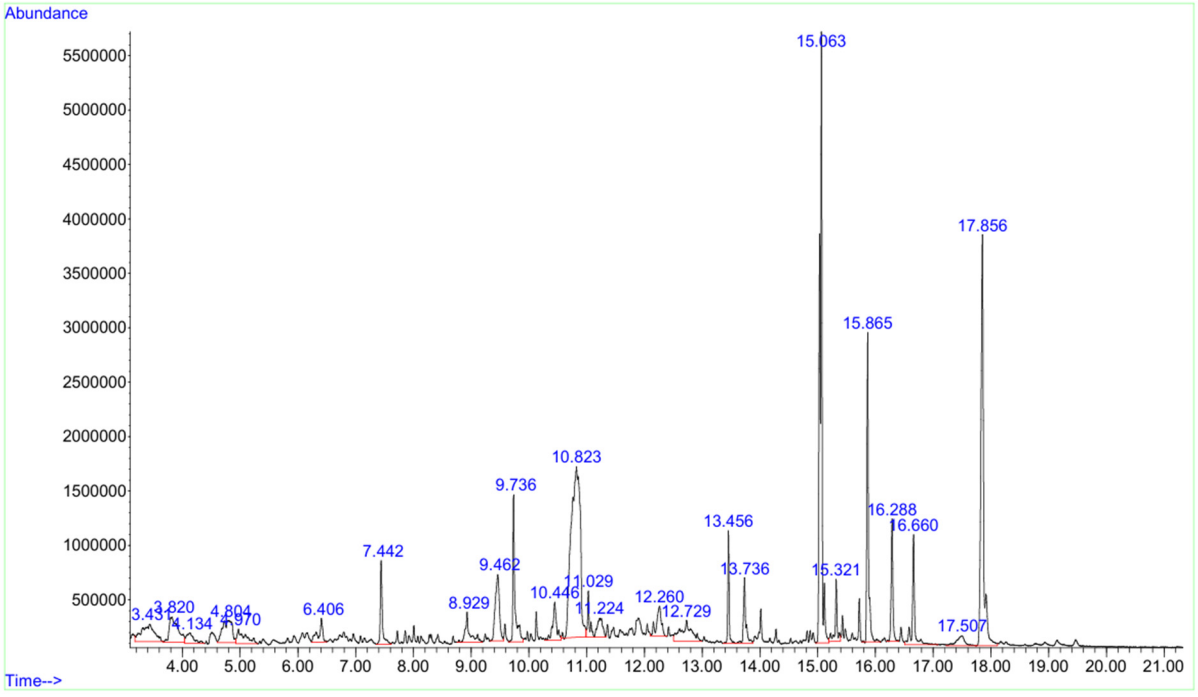


Figure 1. Gas Chromatography–Mass Spectrophotometry spectra of peel extract of the *Citrus aurantium.*

3.2. Comparative Molecular Docking Analysis of Bioactive Compounds Against Staphylococcal Enterotoxin B (4C56) and Toxic Shock Syndrome Toxin-1 (3MFG)

Molecular docking of *Citrus aurantium* peel-derived bioactives against SEB (PDB: 4C56) (Table 3; Figure 2a,b) and TSST-1 (PDB: 3MFG) (Table 4; Figure 3a,b) revealed target-dependent binding affinities, with consistently stronger interactions observed for TSST-1 (−8.774 to −4.917 kcal/mol) compared to SEB (−6.477 to −2.940 kcal/mol). This differential susceptibility may reflect structural differences in the superantigen-binding pockets, as staphylococcal enterotoxins exhibit variable amino acid compositions at critical MHC-II- and TCR-binding interfaces despite sharing a conserved two-domain architecture [15]. Neo-inositol demonstrated the strongest dual-target affinity, achieving −8.774 kcal/mol against TSST-1, surpassing clindamycin (−7.936 kcal/mol), likely attributable to its polyhydroxylated structure facilitating extensive hydrogen bonding with TYR90 and GLY88. Notably, MM/GBSA rescoring identified the chromene derivative and auraptenol as the most thermodynamically stable complexes (ΔG_bind up to −46.28 kcal/mol), a finding consistent with the established superiority of MM/GBSA over standard docking scores in accounting for solvent effects and protein flexibility [16]. These coumarin-type scaffolds, which are well-documented constituents of *C. aurantium* peels with established anti-inflammatory and antimicrobial properties [17,18], engaged conserved hydrophobic hotspots (VAL134/LEU136 in SEB; TYR90/PHE89 in TSST-1) supplemented by critical hydrogen bond interaction patterns that parallel those of high-affinity synthetic inhibitors such as nanobodies targeting the SEB–TCR interface [19]. Given that no specific therapeutic interventions currently exist to counteract SEB-mediated pathogenesis [20], the comparable binding profiles of these phytocompounds relative to standard antibiotics support their prioritization as natural anti-virulence leads against toxin-mediated staphylococcal diseases in the context of escalating AMR.

Table 3. Lead binding affinities and interaction of *C. aurantium*'s most abundant bioactive compounds docked against the 4C56 active site, along with the standard inhibitors Clindamycin, Nafcillin, and Oxacillin.

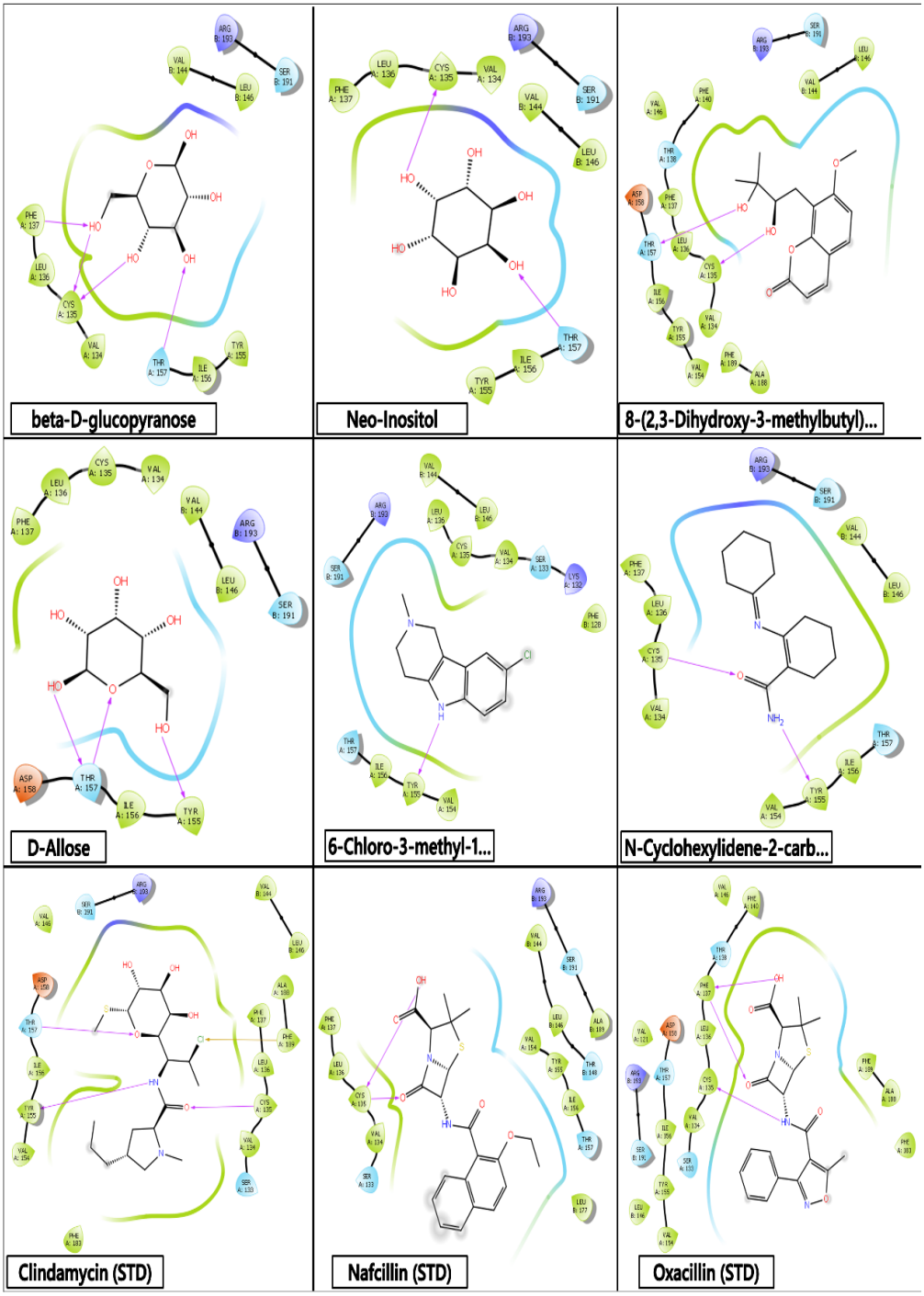
***C. aurantium* Bioactive Compounds (4C56)**	**Docking Scores (Kcal/mol)**	**MMGBSA (ΔGbind)**	**Hydrophobic Amino Acids**	**Hydrogen Bond Interactions**	**Other Interactions**
beta-D-glucopyranose	−6.477	−31.85	VAL 134, VAL 144, LEU 136, LEU 146, ILE 156, TYR 155, CYS 135, PHE 137	PHE 137, CYS 135, THR 157	None
Neo-Inositol	−6.421	−29.38	VAL 134, VAL 144, LEU 136, LEU 146, ILE 156, TYR 155, CYS 135, PHE 137	CYS 135, THR 157	None
8-(2,3-Dihydroxy-3-methylbutyl)-7-methoxy-2H-chromen-2-one	−6.368	−45.71	VAL 134, VAL 154, VAL 144, VAL 146, LEU 136, LEU 146, ILE 156, PHE 137, PHE 140, PHE 189, ALA 188, TYR 155, CYS 135	CYS 135, THR 157	None
D-Allose	−6.037	−37.26	VAL 134, VAL 144, LEU 136, LEU 146, ILE 156, PHE 137, CYS 135, TYR 155	THR 157, TYR 155	None
6-Chloro-3-methyl-1,2,3,4-tetrahydro-gamma-carboline	−5.493	−23.21	VAL 134, VAL 154, VAL 144, LEU 136, LEU 146, ILE 156, PHE 128, CYS 135, TYR 155	TYR 155	None
N-Cyclohexylidene-2-carbamylcyclohex-1-enylamine	−5.344	−38.52	VAL 134, VAL 154, VAL 144, LEU 136, LEU 146, ILE 156, PHE 137, CYS 135, TYR 155	CYS 135, TYR 155	None
Auraptenol	−4.695	−43.73	VAL 134, VAL 154, VAL 144, LEU 136, LEU 146, ILE 156, PHE 137, PHE 189, CYS 135, TYR 155, ALA 188	CYS 135, THR 157	None
3-Methoxyacetophenone	−4.037	−23.89	VAL 134, VAL 154, LEU 146, PHE 137, CYS 135, TYR 155, ALA 188	THR 157	None

Table 3. *Cont.*

C. aurantium Bioactive Compounds (4C56)	Docking Scores (Kcal/mol)	MMGBSA (ΔGbind)	Hydrophobic Amino Acids	Hydrogen Bond Interactions	Other Interactions
Anthracene, 9-methyl-	−3.978	−24.07	VAL 134, VAL 144, LEU 136, LEU 146, ILE 156, PHE 137, PHE 140, CYS 135, TYR 155	None	None
2-Methoxy-4-vinylphenol	−2.940	−30.63	VAL 170, PHE 137, LEU 136, LEU 162, LEU 194, CYS 171	THR 138	None
Clindamycin (STD)	−7.039	−50.09	VAL 134, VAL 154, VAL 144, LEU 136, LEU 146, LEU 109, ILE 156, PHE 137, PHE 183, PHE 189, TYR 155, ALA 188, CYS 135	THR 157, CYS 135	None
Nafcillin (STD)	−6.630	−51.58	VAL 134, VAL 154, VAL 144, LEU 136, LEU 146, LEU 146, LEU 177, ILE 156, PHE 137, PHE 148, CYS 135	CYS 135	None
Oxacillin (STD)	−6.110	−23.32	VAL 121, VAL 134, VAL 146, VAL 154, LEU 136, LEU 146, ILE 156, PHE 137, PHE 183, PHE 189, ALA 188, CYS 135	CYS 135, PHE 137	None

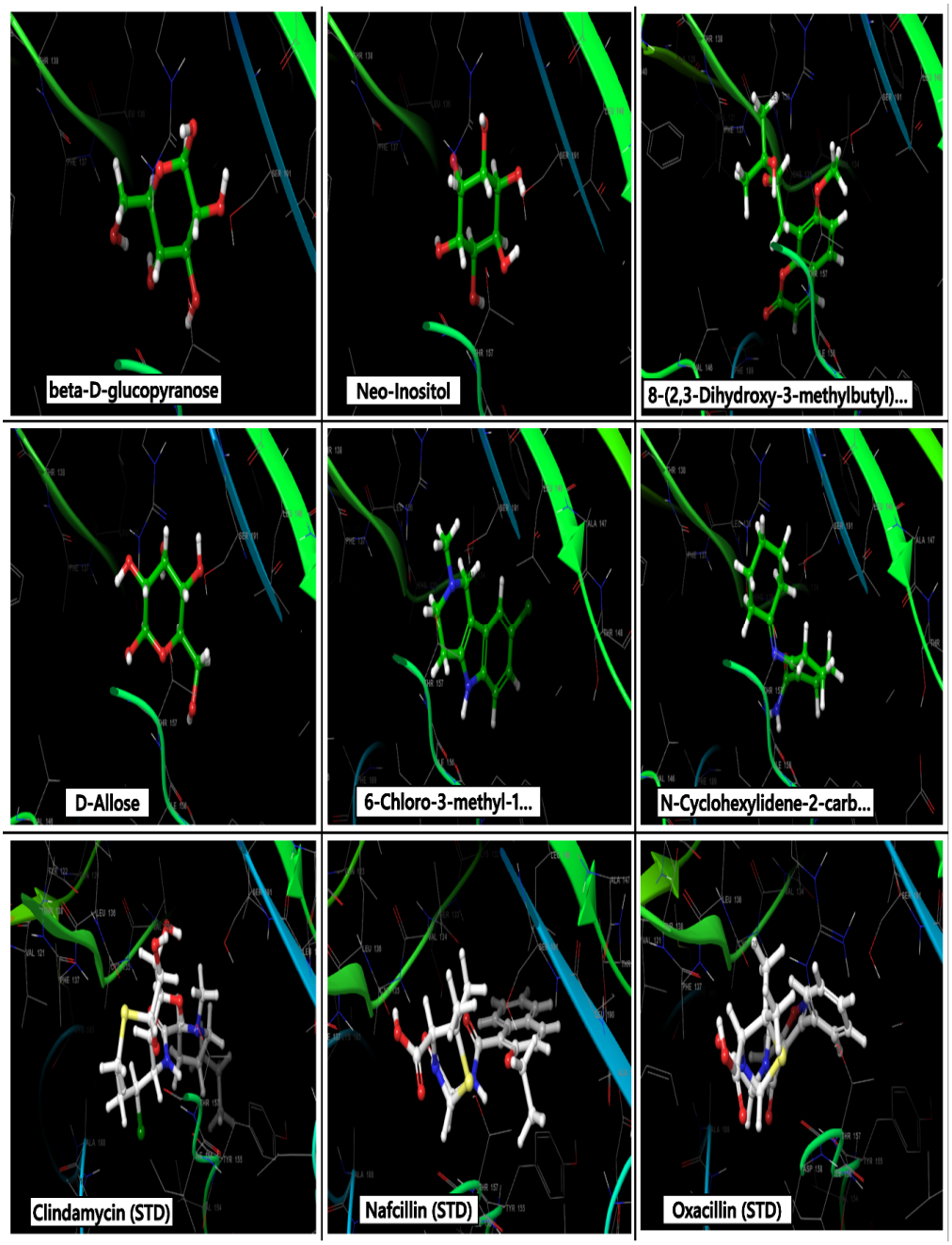
Table 4. Lead binding affinities and interaction of *C. aurantium*'s most abundant bioactive compounds docked against the 3MFG active site, along with the standard inhibitors Clindamycin, Oxacillin, and Nafcillin.

C. aurantium Bioactive Compounds (3MFG)	Docking Scores (Kcal/mol)	MMGBSA (ΔGbind)	Hydrophobic Amino Acids	Hydrogen Bond Interactions	Other Interactions
Neo-Inositol	−8.774	−38.97	ILE 91, TYR 90, PHE 89, PRO 8, VAL 11, ILE 21	TYR 90, GLY 88, PRO 8, GLN 6	None
D-Allose	−7.737	−43.98	TYR 90, PHE 89, PRO 8, VAL 11, ILE 21	TYR 90, GLY 88, PRO 8, VAL 11	None
beta-D-glucopyranose	−6.949	−26.83	ILE 91, TYR 90, PHE 89, PRO 8, VAL 11, ILE 21	TYR 90, GLY 88, PRO 8, GLN 6	None
8-(2,3-Dihydroxy-3-methylbutyl)-7-methoxy-2H-chromen-2-one	−6.852	−46.28	ILE 21, TYR 90, PHE 89, PRO 8, VAL 11, VAL 19, VAL 13, VAL 79, ALA 82	VAL 11, SER 9	None
N-Cyclohexylidene-2-carbamylcyclohex-1-enylamine	−6.293	−38.5	ILE 21, TYR 90, PHE 89, PRO 8, VAL 11, VAL 19, VAL 13, VAL 79, ALA 82	VAL 11, GLY 88, ARG 10	None
Auraptenol	−5.510	−44.2	ILE 21, TYR 90, PHE 89, PRO 8, VAL 11, VAL 19, VAL 79	TYR 90	None
Anthracene, 9-methyl-	−5.334	−35.23	ILE 21, TYR 90, PHE 89, PRO 8, VAL 11, VAL 19, VAL 79	None	None
3-Methoxyacetophenone	−5.285	−30.37	ILE 21, TYR 90, PHE 89, PRO 8, VAL 11, VAL 19, VAL 79	TYR 90	None
6-Chloro-3-methyl-1,2,3,4-tetrahydro-gamma-carboline	−5.280	−31.75	ILE 21, TYR 90, PRO 8, VAL 11, VAL 19, VAL 79, ALA 82	SER 9	None
2-Methoxy-4-vinylphenol	−4.917	−34.42	ILE 21, TYR 90, PHE 89, PRO 8, VAL 11, VAL 19	TYR 90, PRO 8	None
Clindamycin (STD)	−7.936	−48.06	ILE 12, ILE 21, TYR 90, PHE 89, PRO 8, VAL 11, VAL 19, VAL 13, ALA 82	VAL 11, TYR 90, GLY 88, PRO 8, GLN 6, ARG 10	None
Oxacillin (STD)	−7.581	−27.71	ILE 21, ILE 91, TYR 90, PHE 89, PRO 8, VAL 11, VAL 19	TYR 90, GLY 88, PRO 8, SER 9, GLN 6	None
Nafcillin (STD)	−7.034	−46.84	ILE 12, ILE 21, TYR 90, PHE 89, VAL 11, VAL 19, VAL 13, VAL 79, PRO 84, ALA 82	VAL 11, VAL 13, GLY 88, ARG 10	Pi-Pi Stacking



(**a**)

Figure 2. *Cont.*



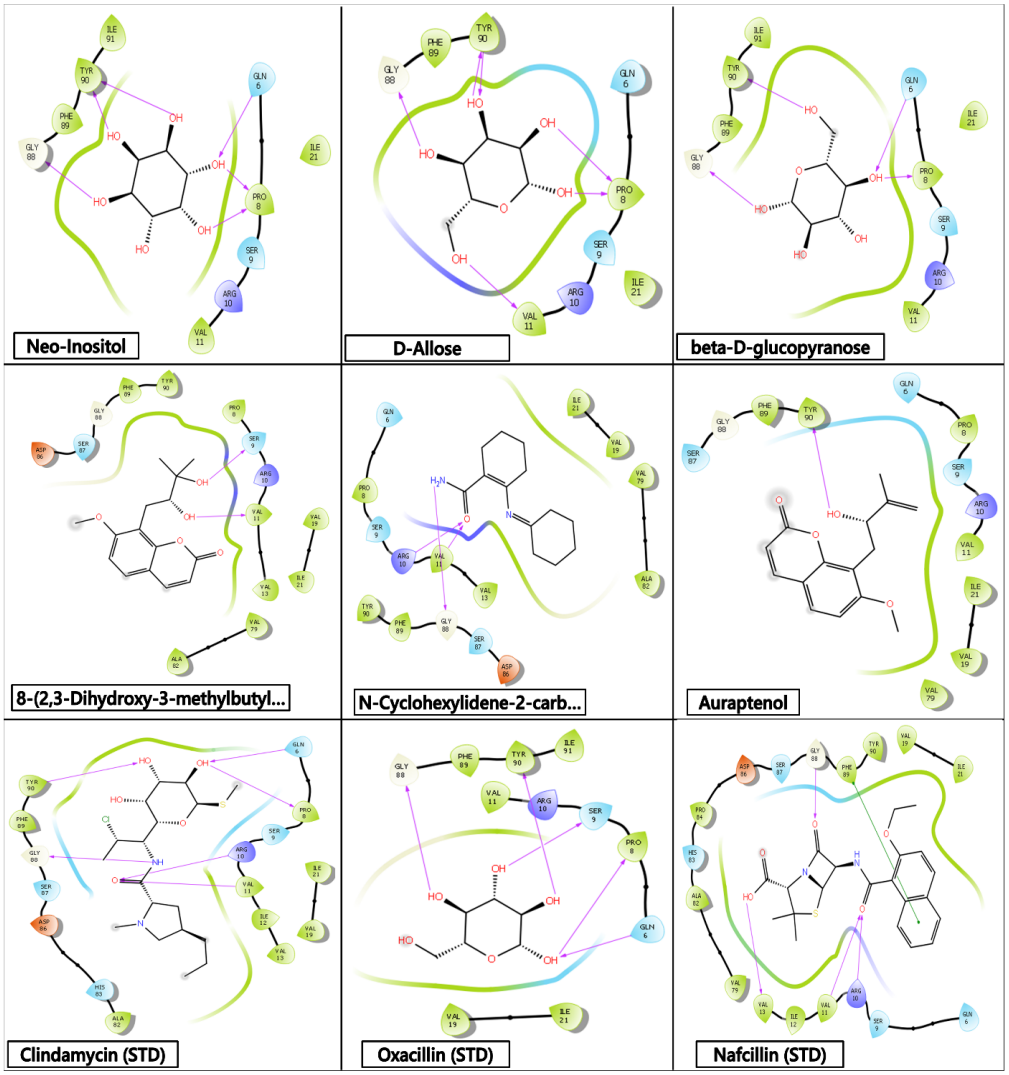
(**b**)

Figure 2. (**a**) 2-Dimensional structure of the top lead compounds of *C. aurantium* L. docked against the 4C56 active site, along with the standard inhibitors Clindamycin, Nafcillin, and Oxacillin. (**b**) 3-dimensional structure of the top lead compounds of *C. aurantium* L. docked against the 4C56 active site, along with the standard inhibitors Clindamycin, Nafcillin, and Oxacillin.

3.3. Comparative Molecular Docking Analysis of Bioactive Compounds Against Protein Targets of Escherichia coli Outer-Membrane Protein A (1BXW) and Topoisomerase IV (3FV5)

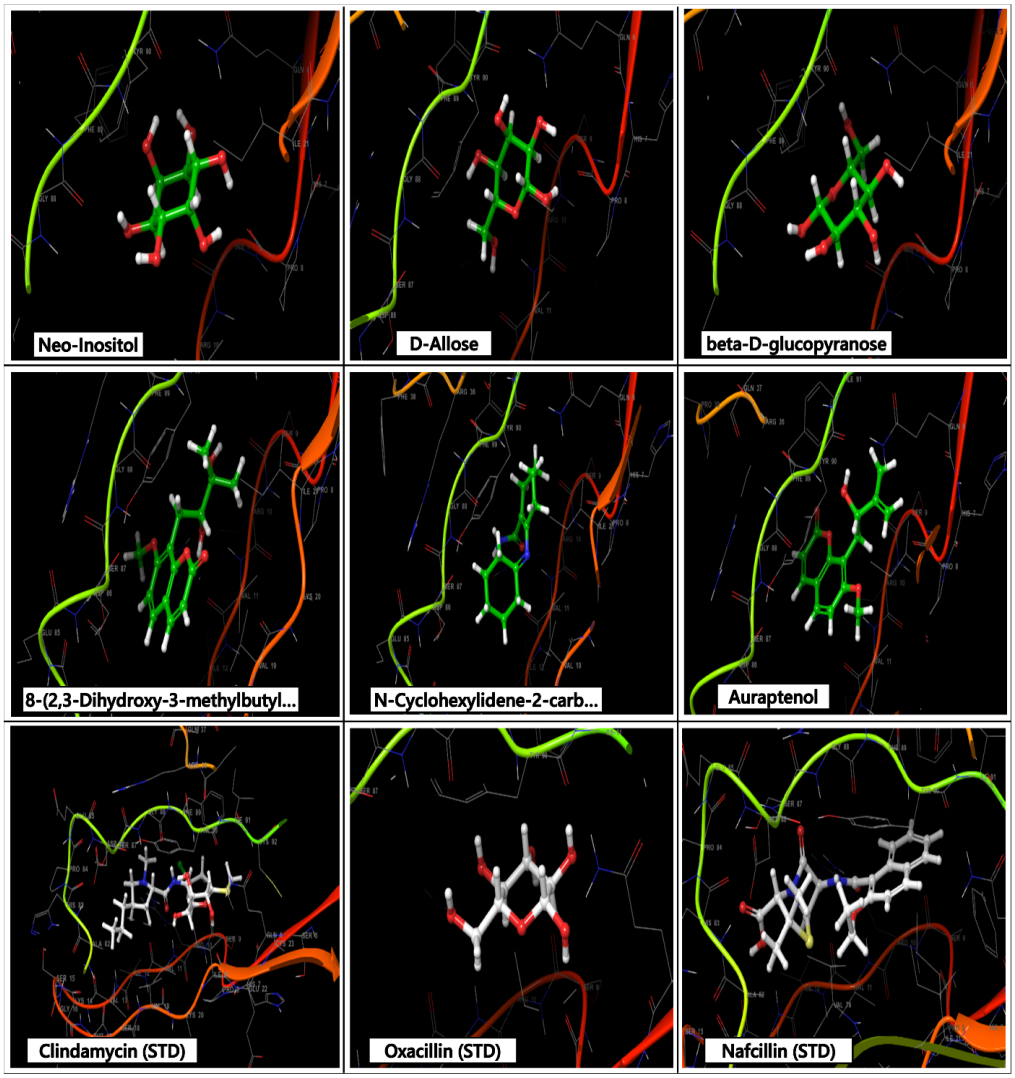
Comparative docking and MM/GBSA analyses against OmpA (1BXW) (Table 5; Figure 4a,b) and Topoisomerase IV (3FV5) (Table 6; Figure 5a,b) revealed complementary antibacterial mechanisms among *C. aurantium* phytochemicals. While polar sugars (neo-inositol, D-allose) achieved the highest docking scores, MM/GBSA consistently favored hydrophobic chromen-2-one derivatives and auraptenol. This aligns with findings that prenylated polyphenolics, including coumarins, exhibit higher docking profiles against bac-

terial targets [21]. OmpA binding involved a hydrophobic pocket (TRP15, LEU13, TYR141), whereas Topoisomerase IV engagement targeted catalytic residues (ASP69, GLY73, ILE90), consistent with reports that plant-derived compounds can simultaneously bind DNA gyrase and Topoisomerase IV complexes through substituent-dependent binding modes [22]. These in silico findings are supported by demonstrated antibacterial and antibiofilm activities of *C. aurantium* essential oil [23]. Generally, these findings support a dual-action model disrupting outer-membrane integrity and DNA topology, and could be a promising multi-target antimicrobial agent.



(**a**)

Figure 3. *Cont.*



(**b**)

Figure 3. (**a**) 2-dimensional structure of the top lead compounds of *C. aurantium* L. docked against the 3MFG active site, along with the standard inhibitors Clindamycin, Oxacillin, and Nafcillin. (**b**) 3-dimensional structure of the top lead compounds of *C. aurantium* L. docked against the 3MFG active site, along with the standard inhibitors Clindamycin, Oxacillin, and Nafcillin.

Table 5. Lead binding affinities and interaction of *C. aurantium*'s most abundant bioactive compounds docked against the 1BXW active site, along with the standard inhibitors Ciprofloxacin and Nitrofurantoin.

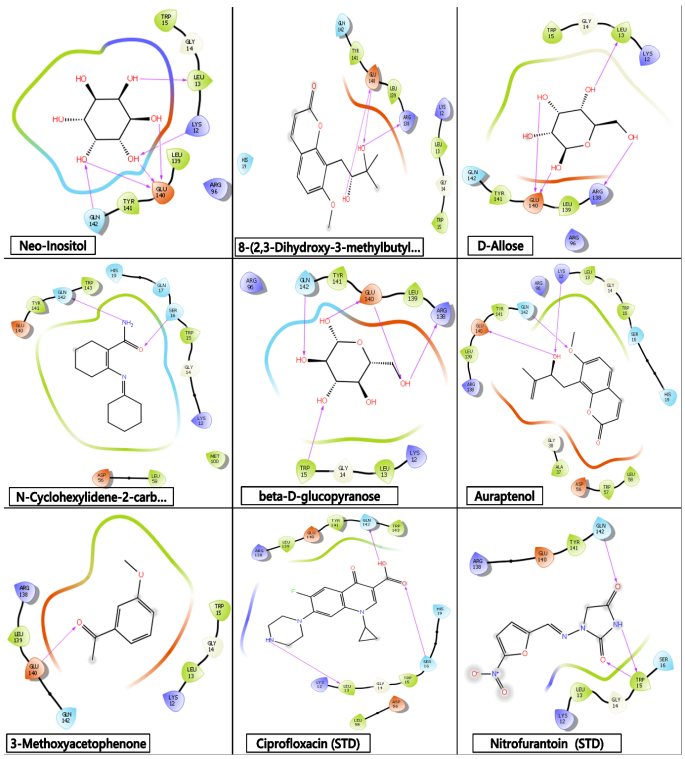
C. aurantium Bioactive Compounds (1BXW)	Docking Scores (Kcal/mol)	MMGBSA (ΔGbind)	Hydrophobic Amino Acids	Hydrogen Bond Interactions	Other Interactions
Neo-Inositol	−7.665	−23.85	TRP 15, LEU 13, LEU 139, TYR 141	LEU 13, LYS 12, GLU 140, GLN 142	None
8-(2,3-Dihydroxy-3-methylbutyl)-7-methoxy-2H-chromen-2-one	−7.023	−45.03	TRP 15, LEU 13, LEU 139, TYR 141	GLU 140, ARG 138	None
D-Allose	−6.615	−22.86	TRP 15, LEU 13, LEU 139, TYR 141	LEU 13, ARG 138, GLU 140	None
N-Cyclohexylidene-2-carbamylcyclohex-1-enylamine	−6.390	−34.18	TRP 15, TRP 143, LEU 58, TYR 141, MET 100	GLN 142, SER 16	None
beta-D-glucopyranose	−5.664	−28.85	TRP 15, LEU 13, LEU 139, TYR 141	GLN 142, GLU 140, ARG 138, TRP 15	None

Table 5. *Cont.*

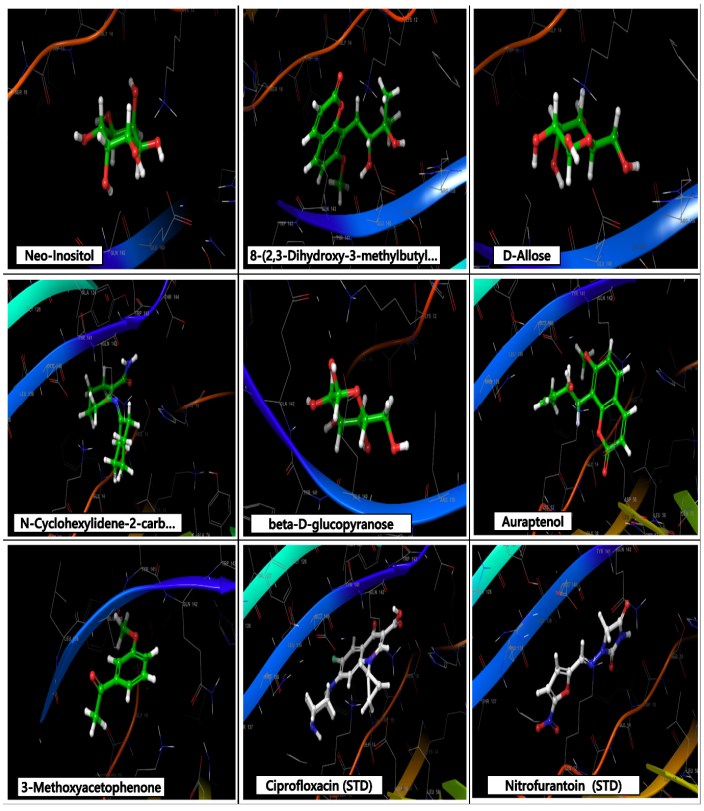
C. aurantium Bioactive Compounds (1BXW)	Docking Scores (Kcal/mol)	MMGBSA (ΔGbind)	Hydrophobic Amino Acids	Hydrogen Bond Interactions	Other Interactions
Auraptenol	−5.325	−41.75	TRP 15, TRP 57, LEU 13, LEU 139, LEU 58, TYR 141, ALA 37	GLU 140, LYS 12, GLN 142	None
3-Methoxyacetophenone	−4.477	−22.91	TRP 15, LEU 13, LEU 139	GLU 140	None
2-Methoxy-4-vinylphenol	−4.371	−32.79	TRP 15, TRP 57, LEU 13, LEU 139, LEU 58, TYR 141, ALA 37	GLU 140, GLN 142	Pi-Cation
6-Chloro-3-methyl-1,2,3,4-tetrahydro-gamma-carboline	−4.158	−33.49	TRP 15, LEU 13, LEU 139	TRP 15	None
Anthracene, 9-methyl-	−3.861	−29.44	TRP 15, LEU 13, LEU 139	None	None
Ciprofloxacin (STD)	−6.855	−55.86	TRP 15, LEU 13, LEU 58, LEU 139, TYR 141, TRP 153	GLN 142, SER 16, LEU 13	None
Nitrofurantoin (STD)	−4.275	−30.74	TRP 15, LEU 13, TYR 141	GLN 142, TRP 15	None

Table 6. Lead binding affinities and interaction of *C. aurantium*'s most abundant bioactive compounds docked against the 3FV5 active site, along with the standard inhibitors Ofloxacin, Levofloxacin, and Ciprofloxacin.

C. aurantium Bioactive Compounds (3FV5)	Docking Scores (Kcal/mol)	MMGBSA (ΔGbind)	Hydrophobic Amino Acids	Hydrogen Bond Interactions	Other Interactions
D-Allose	−6.209	−20.93	ILE 90, MET 74, PRO 75	GLY 73, ASP 69, THR 163	None
beta-D-glucopyranose	−5.716	−27.29	ILE 90, ILE 116, MET 74, PRO 75, VAL 39, VAL 165	GLY 73	None
8-(2,3-Dihydroxy-3-methylbutyl)-7-methoxy-2H-chromen-2-one	−5.139	−37.44	ILE 90, MET 74, PRO 75	ASN 42	None
Neo-Inositol	−4.628	−17.03	ILE 90, MET 74, PRO 75	GLY 73, ASP 69, THR 163, ASN 42	None
Auraptenol	−4.108	−34.8	ILE 90, MET 74, PRO 75, VAL 39	ASN 42	None
2-Methoxy-4-vinylphenol	−3.937	−29.81	ILE 90, MET 74, PRO 75	GLY 73, ASP 69, THR 163	None
3-Methoxyacetophenone	−3.729	−25.02	ILE 90, ILE 116, MET 74, PRO 75, VAL 39, VAL 67, VAL 165	GLY 73, THR 163	None
Anthracene, 9-methyl-	−3.661	−28.89	ILE 90, MET 74, PRO 75	None	None
6-Chloro-3-methyl-1,2,3,4-tetrahydro-gamma-carboline	−2.858	−19.86	ILE 90, ILE 116, MET 74, PRO 75, VAL 165	None	None
N-Cyclohexylidene-2-carbamylcyclohex-1-enylamine	−2.818	−24.35	ILE 90, MET 74, PRO 75	GLU 46	None
Ofloxacin (STD)	−4.388	−42.32	ILE 90, MET 74, PRO 75	GLY 73, ASP 69, THR 163	None
Levofloxacin (STD)	−4.388	−42.32	ILE 90, MET 74, PRO 75	GLY 73, ASP 69, THR 163	None
Ciprofloxacin (STD)	−3.739	−40.07	ILE 90, MET 74, PRO 75	GLY 73, ASP 69	None

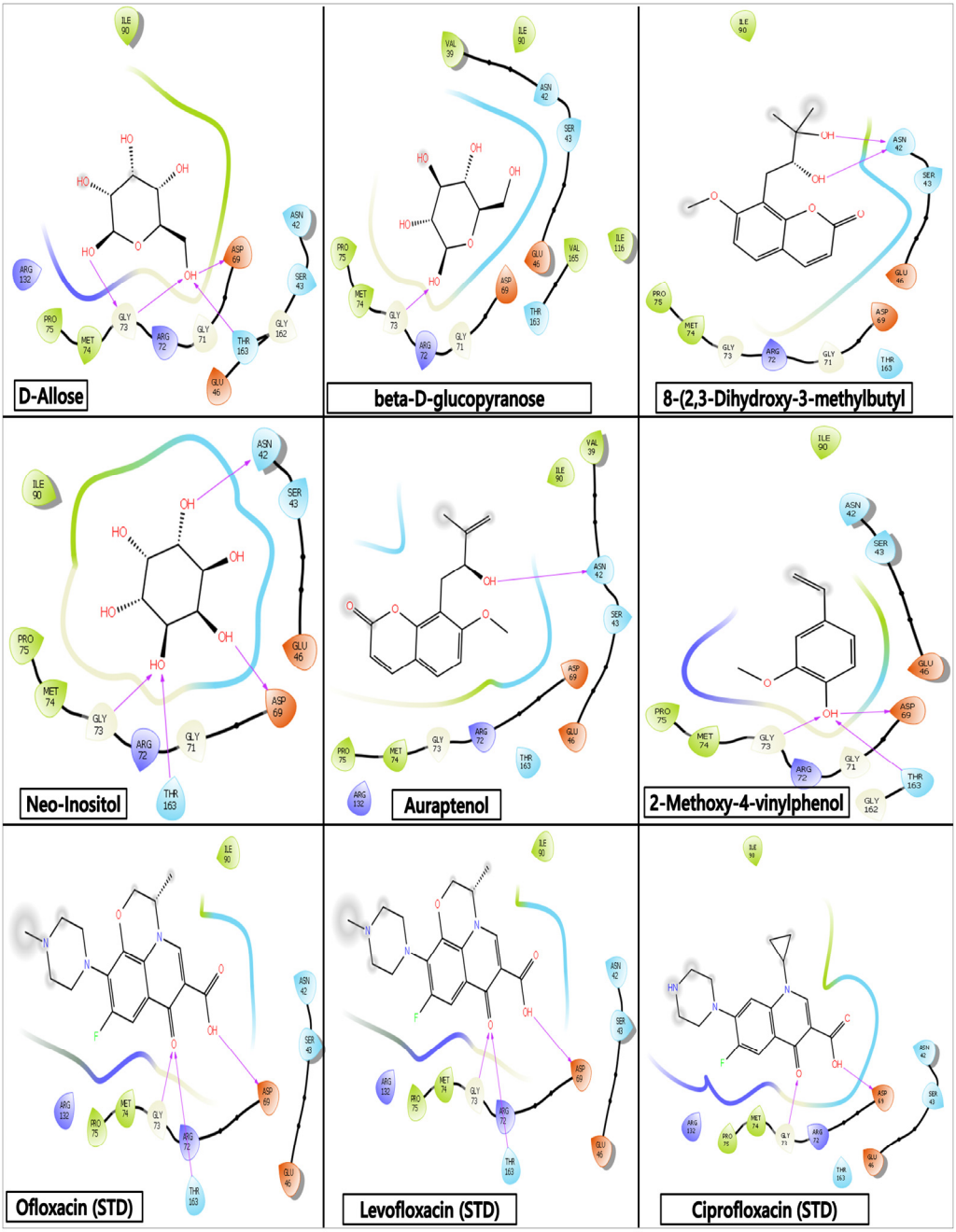


(**a**)



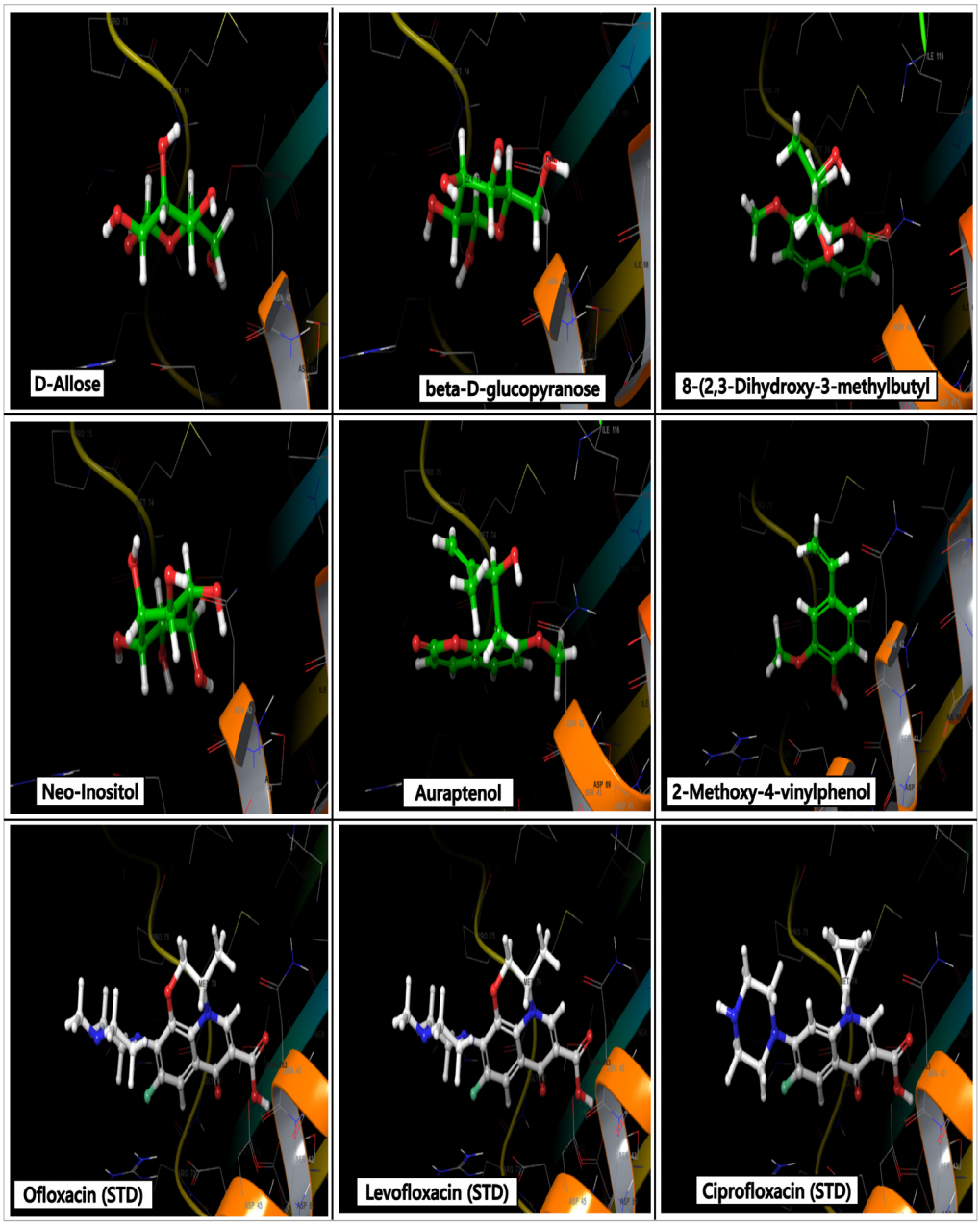
(**b**)

Figure 4. (**a**) 2-dimensional structure of the top lead compounds of *C. aurantium* L. docked against the 1BXW active site, along with the standard inhibitors Ciprofloxacin and Nitrofurantoin. (**b**) 3-dimensional structure of the top lead compounds of *C. aurantium* L. docked against the 1BXW active site, along with the standard inhibitors Ciprofloxacin and Nitrofurantoin.



(**a**)

Figure 5. *Cont.*



(**b**)

Figure 5. (**a**) 2-dimensional structure of the top lead compounds of *C. aurantium* L. docked against the 3FV5 active site, along with the standard inhibitors Ofloxacin, Levofloxacin, and Ciprofloxacin. (**b**) 3-dimensional structure of the top lead compounds of *C. aurantium* L. docked against the 3FV5 active site, along with the standard inhibitors Ofloxacin, Levofloxacin, and Ciprofloxacin.

3.4. Physicochemical Properties, Drug-Likeness, and ADMET/Toxicity Profiling of Citrus aurantium Phytoconstituents

ADMET analysis (Tables 7 and 8) revealed favorable pharmacokinetic profiles for most *C. aurantium* phytochemicals, with high human intestinal absorption predicted for all except neo-inositol, whose high polarity and TPSA limit absorption. BBB permeability varied predictably with polarity, as hydrophobic compounds (chromen-2-one derivative, auraptenol) were permeable while polar sugars were not consistent with broader findings that lipophilic natural products exhibit superior membrane permeation [24]. CYP450 profiling showed selective interactions, particularly for coumarin derivatives, aligning with reports that coumarins demonstrate manageable metabolic profiles with good oral

bioavailability [25]. Toxicity predictions indicated low hepatotoxicity, contrasting with some reference antibiotics [26], though mutagenicity signals in a few compounds warrant experimental validation [27].

Table 7. Pharmacokinetic properties (ADMETox) of the Lead *C. aurantium*'s most abundant bioactive compounds docked against 4C56, 3MFG, 1BXW, and 3FV5 active sites, along with the standard inhibitors.

***C. aurantium* Bioactive Compounds**	**MW**	**HBD**	**HBA**	**LogP**	**TPSA**	**Vd**	**RO5**
beta-D-glucopyranose	180.16	5	6	−3.22	110.38	0.318	0
Neo-Inositol	180.16	6	6	−3.83	121.38	0.231	1
8-(2,3-Dihydroxy-3-methylbutyl)-7-methoxy-2H-chromen-2-one	278.3	2	4	1.28	79.9	0.928	0
D-Allose	180.16	5	6	−2.52	110.38	0.311	0
6-Chloro-3-methyl-1,2,3,4-tetrahydro- gamma-carboline	220.7	1	1	2.91	19.03	3.391	0
N-Cyclohexylidene-2-carbamylcyclohex-1-enylamine	220.31	1	2	2.71	55.45	1.117	0
Auraptenol	260.29	1	4	2.28	59.67	1.579	0
Anthracene, 9-methyl-	192.26	0	0	4.30	0	1.31	1
3-Methoxyacetophenone	150.17	0	2	1.89	26.3	1.24	0
2-Methoxy-4-vinylphenol	150.17	1	2	2.04	29.46	0.39	0
Clindamycin (STD)	424.98	4	8	0.72	102.26	0.77	0
Nafcillin (STD)	414.48	2	5	6	95.94	0.202	0
Oxacillin (STD)	401.44	2	8	2.22	112.74	0.163	0
Ciprofloxacin (STD)	331.34	2	5	1.98	74.57	1.827	0
Nitrofurantoin (STD)	238.16	1	6	0.86	118.05	0.705	0
Ofloxacin (STD)	361.37	1	6	1.55	75.01	1.497	0
Levofloxacin (STD)	361.37	1	6	1.55	75.01	1.387	0

MW = Molecular weight, **HBD** = number of hydrogen bond donors, **HBA** = number of hydrogen bond acceptors, **LogP** = octanol/water partition coefficient, **TPSA** = topological polar surface area, **Vd** = volume of distribution, **RO5** = Lipinski rule of five.

3.5. Antibacterial Potency of Ethanolic Extract of Citrus aurantium Peels

The antibacterial activity of the ethanolic peel extract of *Citrus aurantium* was evaluated at 5 mg/mL and 10 mg/mL against *S. aureus* and *E. coli*, with ciprofloxacin as the control (Figure 6). For *S. aureus*, the extract produced higher inhibition zones of 25.11 ± 0.10 mm at 10 mg/mL, compared to 30.41 ± 0.01 mm for ciprofloxacin. Similarly, *E. coli* showed inhibition zones of 23.04 ± 0.04 mm at 10 mg/mL against the control (30.38 ± 0.19 mm). Statistically, the antibacterial activity of the extract at both concentrations was significantly different from the control ($p < 0.05$) for both organisms. Additionally, a significant increase ($p < 0.05$) in inhibition was observed between 5 mg/mL and 10 mg/mL concentration, confirming a dose-dependent effect. Higher *S. aureus* susceptibility is likely due to the absence of an outer-membrane barrier [28]. The observed dose-dependent inhibition aligns with findings that citrus essential oils exhibit concentration-dependent bactericidal effects mediated through membrane permeability disruption [29]. These results corroborate the findings of Kačániová [23] that *C. aurantium* extracts possess broad antimicrobial potential, which is attributed to phenolics, flavonoids, and terpenes.

Table 8. Pharmacokinetic properties (ADMETox) of the lead *C. aurantium*'s most abundant bioactive compounds docked against 4C56, 3MFG, 1BXW, and 3FV5 active sites, along with the standard inhibitors.

C. aurantium Bioactive Compounds	HIA	P-gp (Substrate/Inhibitor)	BBB	CYP1A2 (Substrate/Inhibitor)	CYP2C19 (Substrate/Inhibitor)	CYP2C9 (Substrate/Inhibitor)	CYP2D6 (Substrate/Inhibitor)	CYP3A4 (Substrate/Inhibitor)	Hepatotoxicity	Carcinogenicity	Mutagenicity	Cytotoxicity
beta-D-glucopyranose	High	Non-Substrate/Non-Inhibitor	BBB+	Non-Substrate/Non-Inhibitor	Non-Substrate/Non-Inhibitor	Non-Substrate/Non-Inhibitor	Non-Substrate/Non-Inhibitor	Non-Substrate/Non-Inhibitor	Inactive	Inactive	Inactive	Inactive
Neo-Inositol	Low	Non-Substrate/Non-Inhibitor	BBB−	Non-Substrate/Non-Inhibitor	Non-Substrate/Non-Inhibitor	Non-Substrate/Non-Inhibitor	Non-Substrate/Non-Inhibitor	Non-Substrate/Non-Inhibitor	Inactive	Inactive	Inactive	Inactive
8-(2,3-Dihydroxy-3-methylbutyl)-7-methoxy-2H-chromen-2-one	High	Non-Substrate/Non-Inhibitor	BBB+	Non-Substrate/Inhibitor	Non-Substrate/Non-Inhibitor	Substrate/Non-Inhibitor	Substrate/Non-Inhibitor	Substrate/Non-Inhibitor	Inactive	Inactive	Active	Inactive
D-Allose	High	Non-Substrate/Non-Inhibitor	BBB−	Non-Substrate/Non-Inhibitor	Non-Substrate/Non-Inhibitor	Non-Substrate/Non-Inhibitor	Non-Substrate/Non-Inhibitor	Non-Substrate/Non-Inhibitor	Inactive	Inactive	Inactive	Inactive
6-Chloro-3-methyl-1,2,3,4-tetrahydro- gamma-carboline	High	Non-Substrate/Non-Inhibitor	BBB+	Substrate/Inhibitor	Substrate/Non-Inhibitor	Substrate/Non-Inhibitor	Substrate/Non-Inhibitor	Substrate/Non-Inhibitor	Inactive	Inactive	Active	Inactive
N-Cyclohexylidene-2-carbamylcyclohex-1-enylamine	High	Non-Substrate/Inhibitor	BBB+	Non-Substrate/Inhibitor	Non-Substrate/Non-Inhibitor	Substrate/Non-Inhibitor	Substrate/Non-Inhibitor	Non-Substrate/Non-Inhibitor	Inactive	Inactive	Inactive	Inactive
Auraptenol	High	Non-Substrate/Non-Inhibitor	BBB+	Substrate/Inhibitor	Substrate/Non-Inhibitor	Substrate/Non-Inhibitor	Substrate/Non-Inhibitor	Non-Substrate/Non-Inhibitor	Inactive	Inactive	Inactive	Inactive
Anthracene, 9-methyl-	High	Substrate/Non-Inhibitor	BBB+	Substrate/Inhibitor	Substrate/Non-Inhibitor	Substrate/Inhibitor	Substrate/Non-Inhibitor	Non-Substrate/Non-Inhibitor	Inactive	Inactive	Active	Inactive
3-Methoxyacetophenone	High	Non-Substrate/Non-Inhibitor	BBB+	Substrate/Inhibitor	Substrate/Inhibitor	Substrate/Inhibitor	Substrate/Non-Inhibitor	Non-Substrate/Non-Inhibitor	Inactive	Active	Inactive	Inactive
2-Methoxy-4-vinylphenol	High	Non-Substrate/Non-Inhibitor	BBB+	Substrate/Non-Inhibitor	Substrate/Non-Inhibitor	Substrate/Non-Inhibitor	Substrate/Non-Inhibitor	Substrate/Non-Inhibitor	Inactive	Inactive	Inactive	Inactive
Clindamycin (STD)	High	Substrate/Non-Inhibitor	BBB−	Non-Substrate/Non-Inhibitor	Non-Substrate/Non-Inhibitor	Non-Substrate/Non-Inhibitor	Non-Substrate/Non-Inhibitor	Substrate/Non-Inhibitor	Inactive	Inactive	Inactive	Inactive
Nafcillin (STD)	High	Non-Substrate/Non-Inhibitor	BBB−	Non-Substrate/Non-Inhibitor	Non-Substrate/Non-Inhibitor	Non-Substrate/Non-Inhibitor	Non-Substrate/Non-Inhibitor	Non-Substrate/Non-Inhibitor	Active	Inactive	Inactive	Inactive
Oxacillin (STD)	High	Non-Substrate/Non-Inhibitor	BBB−	Non-Substrate/Non-Inhibitor	Non-Substrate/Non-Inhibitor	Non-Substrate/Non-Inhibitor	Non-Substrate/Non-Inhibitor	Non-Substrate/Non-Inhibitor	Inactive	Inactive	Inactive	Inactive
Ciprofloxacin (STD)	High	Substrate/Non-Inhibitor	BBB−	Non-Substrate/Non-Inhibitor	Substrate/Non-Inhibitor	Non-Substrate/Non-Inhibitor	Non-Substrate/Non-Inhibitor	Non-Substrate/Non-Inhibitor	Inactive	Inactive	Active	Inactive
Nitrofurantoin (STD)	High	Non-Substrate/Non-Inhibitor	BBB+	Non-Substrate/Inhibitor	Non-Substrate/Non-Inhibitor	Substrate/Non-Inhibitor	Non-Substrate/Non-Inhibitor	Non-Substrate/Non-Inhibitor	Active	Active	Active	Inactive
Ofloxacin (STD)	High	Substrate/Non-Inhibitor	BBB−	Non-Substrate/Non-Inhibitor	Non-Substrate/Non-Inhibitor	Non-Substrate/Non-Inhibitor	Non-Substrate/Non-Inhibitor	Non-Substrate/Non-Inhibitor	Inactive	Inactive	Active	Inactive
Levofloxacin (STD)	High	Substrate/Non-Inhibitor	BBB−	Non-Substrate/Non-Inhibitor	Non-Substrate/Non-Inhibitor	Non-Substrate/Non-Inhibitor	Non-Substrate/Non-Inhibitor	Non-Substrate/Non-Inhibitor	Inactive	Inactive	Active	Inactive

HIA = Human intestinal absorption, **BBB** = blood–brain barrier penetration, P-gp = P-glycoprot.

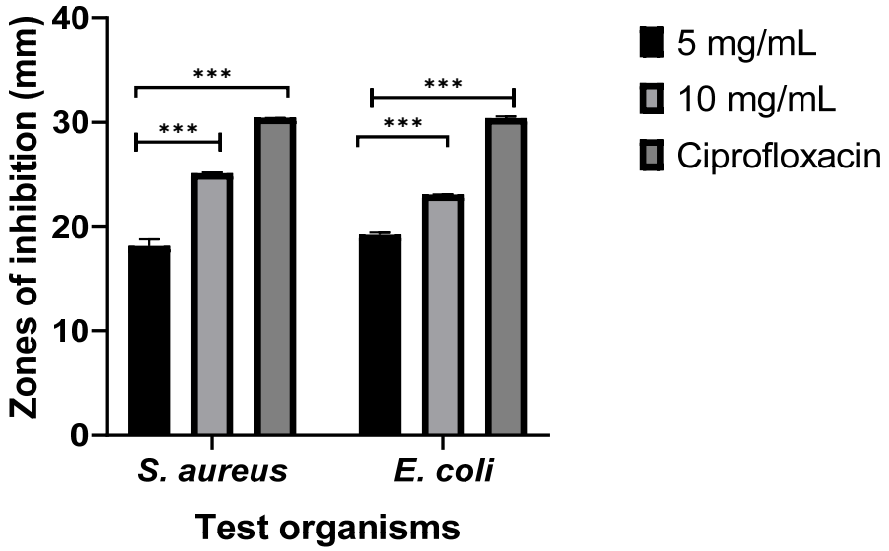


Figure 6. Antibacterial potency of ethanolic extract of *Citrus aurantium* peels. *** showed a significant ($p < 0.05$) difference in zone of inhibition.

4. Conclusions

In conclusion, this study has demonstrated that the ethanolic peel extract of *Citrus aurantium* is a potent reservoir of bioactive phytochemicals, especially flavonoids and coumarin derivatives, with notable antimicrobial properties. Our comprehensive in vitro and in silico analyses have revealed a multi-target mechanism, where key compounds, including chromene derivatives and auraptenol, demonstrated impressive binding stability against staphylococcal toxins and bacterial proteins, further supported by favorable ADMET profiles. While the antibacterial activity of the extract may be lower than that of conventional antibiotics, it exhibited significant efficacy, particularly against *S. aureus*. This evidence strongly advocates for the potential of *C. aurantium* peel as a natural anti-virulence and antimicrobial agent.

To propel these promising phytocompounds toward therapeutic applications and effectively address the rising challenge of antimicrobial resistance, further studies on purification of active compounds in *C. aurantium* peel, experimental validation, including in vivo and more in vitro studies, and toxicity evaluations are essential.

Author Contributions: Conceptualization, K.O.A. and B.K.O.; methodology, B.T.O. and K.O.A.; software, B.T.O.; validation, T.O.A., B.T.O. and B.K.O.; formal analysis, K.O.A.; investigation, B.K.O.; resources, T.O.A.; data curation, B.K.O.; writing—original draft preparation, B.K.O.; writing—review and editing, K.O.A.; visualization, B.T.O.; supervision, K.O.A.; project administration, T.O.A.; funding acquisition, B.K.O. and K.O.A. All authors have read and agreed to the published version of the manuscript.

Funding: This research received no external funding.

Institutional Review Board Statement: Not applicable.

Informed Consent Statement: Not applicable.

Data Availability Statement: The raw data generated during the study is available from the author.

Acknowledgments: The authors would like to acknowledge the administrative and technical support given by O. K. Alao, the Head of Department, Natural Science, Precious Cornerstone University, Ibadan. Also, we acknowledge ChatGPT.com (https://chatgpt.com/, accessed on 1 March 2026), which was used during study design and during the preparation of this manuscript; the author(s)

used it for the purposes of summarizing ideas and grammar checking. The authors have reviewed and edited the output and take full responsibility for the content of this publication.

Conflicts of Interest: The authors declare no conflicts of interest.

References

1. Antimicrobial Resistance Collaborators. Global burden of bacterial antimicrobial resistance in 2019: A systematic analysis. *Lancet* **2022**, *399*, 629–655. [CrossRef] [PubMed]
2. Caniça, M.; Manageiro, V.; Abriouel, H.; Moran-Gilad, J.; Franz, C.M.A.P. Antibiotic resistance in foodborne bacteria. *Trends Food Sci. Technol.* **2019**, *84*, 41–44. [CrossRef]
3. Founou, L.L.; Founou, R.C.; Essack, S.Y. Antimicrobial resistance in the farm-to-plate continuum: More than a food safety issue. *Future Sci. OA* **2021**, *7*, FSO692. [CrossRef] [PubMed]
4. Sagar, P.; Aseem, A.; Banjara, S.K.; Veleri, S. The role of food chain in antimicrobial resistance spread and one health approach to reduce risks. *Int. J. Food Microbiol.* **2023**, *391–393*, 110148. [CrossRef]
5. Hadi, S.T.; Mahmed, A.M.; Sulieman, A.M.E. Chemical composition and active compounds in bitter orange (*Citrus aurantium*) peels. *Funct. Food Sci.* **2025**, *5*, 328–339. [CrossRef]
6. Alzand, K. *Citrus aurantium* L. peels and seeds: Phytochemical screening and antibacterial activity. *New Mater. Compd. Appl.* **2024**, *8*, 75. [CrossRef]
7. Gomathi, D.; Kalaiselvi, M.; Ravikumar, G.; Devaki, K.; Uma, C. GC–MS analysis of bioactive compounds from the whole plant ethanolic extract of *Evolvulus alsinoides* (L.) L. *J. Food Sci. Technol.* **2015**, *52*, 1212–1217. [CrossRef]
8. Abishad, P.; Niveditha, P.; Unni, V.; Vergis, J.; Kurkure, N.V.; Chaudhari, S.; Rawool, D.B.; Barbuddhe, S.B. In silico molecular docking and in vitro antimicrobial efficacy of phytochemicals against multi-drug-resistant enteroaggregative *Escherichia coli* and non-typhoidal *Salmonella* spp. *Gut Pathog.* **2021**, *13*, 46. [CrossRef]
9. Morris, G.M.; Huey, R.; Lindstrom, W.; Sanner, M.F.; Belew, R.K.; Goodsell, D.S.; Olson, A.J. AutoDock4 and AutoDockTools4: Automated docking with selective receptor flexibility. *J. Comput. Chem.* **2009**, *30*, 2785–2791. [CrossRef]
10. Banerjee, P.; Eckert, A.O.; Schrey, A.K.; Preissner, R. ProTox-II: A webserver for the prediction of toxicity of chemicals. *Nucleic Acids Res.* **2018**, *46*, W257–W263. [CrossRef]
11. Reeves, D.S. Antibiotic assays. In *Medical Bacteriology: A Practical Approach*; Hawkey, P.M., Lewis, D.A., Eds.; IRL Press: Oxford, UK, 1989; pp. 195–221.
12. Ashraf, S.A.; Al-Shammari, E.; Hussain, T.; Tajuddin, S.; Panda, B.P. In-vitro antimicrobial activity and identification of bioactive components using GC–MS of commercially available essential oils in Saudi Arabia. *J. Food Sci. Technol.* **2017**, *54*, 3948–3958. [CrossRef]
13. Ajayi, O.S.; Olusegun, I.I. Antibacterial potential of orange (*Citrus aurantium*) peels against selected Gram-positive and Gram-negative bacteria isolated from FUTA Botanical Garden soil. *Path Sci.* **2023**, *9*, 5001–5016. [CrossRef]
14. Benayad, O.; Bouhrim, M.; Tiji, S.; Kharchoufa, L.; Addi, M.; Drouet, S.; Hano, C.; Lorenzo, J.M.; Bendaha, H.; Bnouham, M.; et al. Phytochemical profile, α-glucosidase, and α-amylase inhibition potential and toxicity evaluation of extracts from *Citrus aurantium* (L) peel, a valuable by-product from Northeastern Morocco. *Biomolecules* **2021**, *11*, 1555. [CrossRef] [PubMed]
15. Zeng, C.; Liu, Z.-X.; Han, Z. Structure of staphylococcal enterotoxin N: Implications for binding properties to its cellular proteins. *Int. J. Mol. Sci.* **2019**, *20*, 5921. [CrossRef]
16. Wang, E.; Sun, H.; Wang, J.; Wang, Z.; Liu, H.; Zhang, J.H.; Hou, T. End-point binding free energy calculation with MM/PBSA and MM/GBSA: Strategies and applications in drug design. *Chem. Rev.* **2019**, *119*, 9478–9508. [CrossRef]
17. Bibak, B.; Shakeri, F.; Barreto, G.; Keshavarzi, Z.; Sathyapalan, T.; Sahebkar, A. A review of the pharmacological and therapeutic effects of auraptene. *Biofactors* **2019**, *45*, 867–879. [CrossRef]
18. Tayarani-Najaran, Z.; Tayarani-Najaran, N.; Eghbali, S. A review of auraptene as an anticancer agent. *Front. Pharmacol.* **2021**, *12*, 698352. [CrossRef] [PubMed]
19. Zong, X.; Liu, P.; Wang, Z.; Zhu, H.; Zhong, C.; Zhong, P.; Jiang, H.; Liu, J.-Y.; Ma, Z.; Liu, X.; et al. Structural insights into the binding of nanobodies to the staphylococcal enterotoxin B. *Int. J. Biol. Macromol.* **2024**, *275*, 133957. [CrossRef]
20. Fan, H.; Zhao, L.; Wang, W.; Yu, F.; Jing, H.; Yang, Y.; Zhang, X.; Zhao, Z.; Gou, Q.; Zhang, W.; et al. A highly neutralizing human monoclonal antibody targeting a novel linear epitope on staphylococcal enterotoxin B. *Hum. Vaccines Immunother.* **2024**, *20*, 2360338. [CrossRef]
21. Setzer, M.S.; Sharifi-Rad, J.; Setzer, W.N. The search for herbal antibiotics: An in-silico investigation of antibacterial phytochemicals. *Antibiotics* **2016**, *5*, 30. [CrossRef]
22. Alov, P.; Al Sharif, M.; Najdenski, H.; Pencheva, T.; Tsakovska, I.; Zaharieva, M.; Pajeva, I. New potential pharmacological targets of plant-derived hydroxyanthraquinones from *Rubia* spp. *Molecules* **2022**, *27*, 3274. [CrossRef]

23. Kačániová, M.; Galovičová, L.; Ivanišová, E.; Vukovic, N.L.; Štefániková, J.; Valková, V.; Borotová, P.; Žiarovská, J.; Terentjeva, M.; Felšöciová, S.; et al. Biological activity and antibiofilm molecular profile of Citrus aurantium essential oil and its application in a food model. *Molecules* **2020**, *25*, 3956. [CrossRef]
24. Mohanraj, K.; Karthikeyan, B.S.; Vivek-Ananth, R.P.; Chand, R.P.B.; Aparna, S.R.; Mangalapandi, P.; Samal, A. IMPPAT: A curated database of Indian Medicinal Plants, Phytochemistry and Therapeutics. *Sci. Rep.* **2017**, *8*, 4329. [CrossRef]
25. Żołek, T.; Maciejewska, D. Theoretical evaluation of ADMET properties for coumarin derivatives as compounds with therapeutic potential. *Eur. J. Pharm. Sci.* **2017**, *100*, 215–226.
26. Park, S.M.; Choi, M.S.; Kim, S.; Hyun, J.; Han, H.Y.; Choi, H.S.; Oh, J.-H.; Kim, S.K. Hepa-ToxMOA: A pathway-screening method for evaluating cellular stress and hepatic metabolic-dependent toxicity of natural products. *Sci. Rep.* **2024**, *14*, 4319. [CrossRef] [PubMed]
27. Odhiambo, D.O.; Omosa, L.K.; Njagi, E.C.; Kithure, J.G.N.; Wekesa, E.N. In-silico pharmacokinetics ADME/Tox analysis of phytochemicals from genus Dracaena for their therapeutic potential. *Sci. Afr.* **2025**, *29*, e02796. [CrossRef]
28. Fratianni, F.; Cozzolino, A.; De Feo, V.; Coppola, R.; Ombra, M.N.; Nazzaro, F. Polyphenols, antioxidant, antibacterial, and biofilm inhibitory activities of peel and pulp of *Citrus medica* L., *Citrus bergamia*, and *Citrus medica* cv. Salò cultivated in Southern Italy. *Molecules* **2019**, *24*, 4577. [CrossRef] [PubMed]
29. Song, X.; Liu, T.; Wang, L.; Liu, L.; Li, X.; Wu, X. Antibacterial effects and mechanism of mandarin (*Citrus reticulata* L.) essential oil against Staphylococcus aureus. *Molecules* **2020**, *25*, 4956. [CrossRef]

Disclaimer/Publisher's Note: The statements, opinions and data contained in all publications are solely those of the individual author(s) and contributor(s) and not of MDPI and/or the editor(s). MDPI and/or the editor(s) disclaim responsibility for any injury to people or property resulting from any ideas, methods, instructions or products referred to in the content.